BRL

406 825

REPORT NO. 1200
APRIL 1963

FARADAY ROTATION NEAR THE TRANSVERSE REGION OF THE IONOSPHERE

George A. Dulk

RDT & E Project No. 1A011001B021

BALLISTIC RESEARCH LABORATORIES

ABERDEEN PROVING GROUND, MARYLAND

(4) 2.60

(5) 104 500

BALLISTIC RESEARCH LABORATORIES

(14) REPORT NO. 1200

(11) APR[redacted]63,

(6) FARADAY ROTATION NEAR THE TRANSVERSE REGION OF THE IONOSPHERE,

(7) NA
(8) NA
(9) NA

(10) by George A. Dulk,

Ballistic Measurements Laboratory

(12) 32 p. (13) NA (15) NA
(17-19) NA

(20) 4

(21) NA

(Partially Supported by the Defense Atomic Support Agency, WEB No. 07.013)

(16) RDT & E Project [redacted] 1A011001B021

ABERDEEN PROVING GROUND, MARYLAND

BALLISTIC RESEARCH LABORATORIES

REPORT NO. 1200

GADulk/bj
Aberdeen Proving Ground, Md.
April 1963

FARADAY ROTATION NEAR THE TRANSVERSE REGION OF THE IONOSPHERE

ABSTRACT

It is shown that some of the equations usually used to describe Faraday rotation are incorrect for the case of propagation through an anisotropic magnetic field when the cosine of the angle between the magnetic field and the wave normal changes sign along the ray path. Such a case is common when transmissions are from a high altitude satellite in the region of the ionosphere where the direction of propagation is nearly perpendicular to the earth's magnetic field. Use of the uncorrected equations can result in misinterpretation of the data. The corrected equations are given and are shown to be consistent with measured Faraday rotation. With the corrected equations used in a ray tracing program, an analysis is made of errors resulting from the use of several approximations near the transverse region. The approximations investigated are: (1) quasi-longitudinal propagation, (2) straight line propagation, and (3) use of an effective ionospheric height.

406825

INTRODUCTION

During the summer of 1962, recordings were made of the satellite radio signals from the Transit 4A satellite at a low latitude receiving station. During the analysis of the Faraday rotation of these signals, it was found that sample calculations with a ray tracing program gave results which were not always consistent with the measured data. It was found that whenever the earth's magnetic field is perpendicular to the ray path at some point between the transmitter and receiver, the equations generally used to describe the Faraday rotation are incorrect. In Section I of this report the correct equations are derived, and in Section II they are applied to analyze errors resulting from the use of several different approximations.

I. EQUATIONS OF FARADAY ROTATION

Whenever a receiving station is at a sufficiently low geomagnetic latitude (less than about 40°), there is a portion of the sky where radio signals from a satellite propagate perpendicular to the earth's magnetic field at some point along the ray path. This portion of the sky is referred to in this paper as the "transverse region", and the point of perpendicularity along the ray path as the "transverse point". When the satellite is on one side of the transverse region, there is a component of the earth's magnetic field parallel to the direction of propagation, as in the case of vertically downward propagation in the northern magnetic hemisphere. When the satellite is on the other side of the transverse region, the magnetic field has a component antiparallel to the direction of propagation (parallel, but in the opposite direction), as in the case of vertically downward propagation in the southern magnetic hemisphere.

To understand propagation near the transverse region, it is necessary to consider the polarizations of the "ordinary" and "extraordinary" magnetoionic modes and the resultant wave. By definition, the ordinary ray is that which is unaffected by the magnetic field when propagation is transverse to the field. When there is a longitudinal component of the field, collision effects are negligible, and the wave frequency is higher than the gyromagnetic frequency, the ordinary wave is less affected by the magnetic field than is

the extraordinary wave. For purely longitudinal propagation, the two waves are circularly polarized with opposite sense of rotation. Referring to Figure 1A, the direction and magnitude of the force felt by a charge, q, moving perpendicular to the magnetic field is given by the equation $\vec{F} = q\,\vec{v} \times \vec{B}$. Letting $\vec{v} = v\,\vec{j}$ and $\vec{B} = B\,\vec{k}$, then $F_i = q(v_j B_k - v_k B_j)$ or $\vec{F} = q\,v\,B\,\vec{i}$, so the charge would circle counterclockwise as shown. An electron would circle in the opposite direction, (clockwise) as shown in Figure 1B (where the magnetic field is directed into the paper).

Consider two circularly polarized waves of opposite sense of rotation propagating parallel to the magnetic field. Again referring to Figure 1B, it can be visualized that the electrons have more chance to be influenced by a clockwise wave than by a counterclockwise wave, and that the interaction is a maximum when the wave frequency is equal to the gyromagnetic frequency. Hence the clockwise wave is more affected by the magnetic field, and therefore is the extraordinary wave.

To determine the direction of Faraday rotation, let us consider the ordinary and extraordinary waves at two planes which are perpendicular to the wave normal and a distance $d\vec{\ell}$ apart along the wave normal. This situation is depicted in Figure 1C. At plane A at time t_o, let the E vectors of the two waves ($\vec{E}_o$ and $\vec{E}_x$) be in the direction of $\vec{i}$. Both the ordinary and extraordinary waves are circularly polarized, so that as time progresses, $\vec{E}_o$ rotates counterclockwise at the wave frequency, $\vec{E}_x$ rotates clockwise, and the resultant $\vec{E}$ is plane polarized in the plane of $\vec{i}$ and $d\vec{\ell}$. At plane B at time t_o, the phase of $\vec{E}_o$ is lagging (clockwise) by an angle ϕ_o and $\vec{E}_x$ is lagging (counterclockwise) by an angle ϕ_x. (Viewing $\vec{E}_o$ at time t_o, it is seen that it describes a right-hand helix in space, and $\vec{E}_x$ describes a left-hand helix.) However, since the wave length of the extraordinary wave is greater than that of the ordinary wave, $\phi_x < \phi_o$. The resultant $\vec{E}$ is in a direction making an angle $\phi = \frac{\phi_o - \phi_x}{2}$ clockwise from $\vec{i}$. As time progresses, $\vec{E}_o$ rotates counterclockwise and $\vec{E}_x$ rotates clockwise at the wave frequency so that $\vec{E}$ is plane polarized with the polarization plane lagging (clockwise) by an angle ϕ from its position at plane A. Therefore, the plane of $\vec{E}$ is twisted clockwise in space, so we may say that the total Faraday rotation is

FIGURE IA

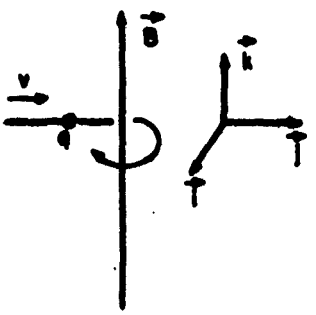

FIGURE IB

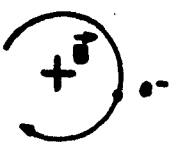

FIGURE IC

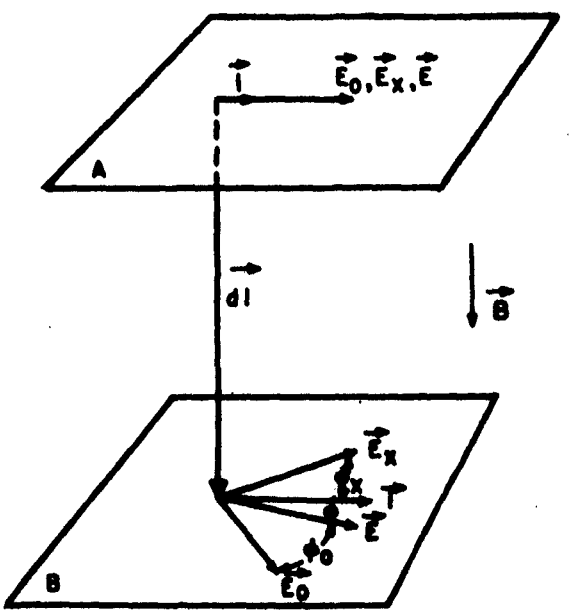

FIGURE ID

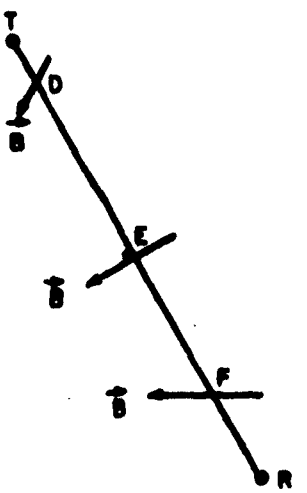

FIGURE 1. FOR EXPLANATION SEE TEXT.

clockwise when propagation is parallel to the magnetic field. In the opposite case, when propagation is antiparallel to the magnetic field, the total rotation of a downcoming ray is counterclockwise.

It may be noted that in the case of parallel propagation, if the electron density or longitudinal component of the magnetic field is decreasing along the ray path, there will be decreasing amounts of total Faraday rotation, so the plane of the $\vec{E}$ vector at the ground will rotate counterclockwise as viewed from the transmitter.

Whenever the propagation is transverse to the magnetic field, the above analysis is not valid since the ordinary and extraordinary waves are no longer circularly polarized. For purely transverse propagation they are linearly polarized in space quadrature. The resultant wave is then circularly polarized and Faraday rotation cannot be defined simply as the rotation of the plane of polarization. However, in the ionosphere, only in the special case of a receiving station directly on the magnetic equator can there be transverse propagation along the entire ray path from a transmitter.

In the more general case, consider a receiving station in the northern hemisphere at a sufficiently low latitude that transverse propagation can exist, and consider a transmitter fixed in the transverse region of the sky. There will be only one point along the ray path where propagation is purely transverse. Above this point the propagation will have a component parallel to the magnetic field, while below the point there is a component antiparallel to the field. (In the actual case described later, the receiving station was at 16°N geomagnetic latitude and a 54 mc transmitter was at an altitude of 970 km. The transverse point was at an altitude of 360 km. At 954 km the angle between the ray direction and the magnetic field was 83.2° at 360 km the angle was 90°, and at 109 km the angle was 92.9°.) Figure 1D depicts the magnetic field geometry in such a case where a linearly polarized signal is transmitted from T. At point D there is a parallel component of the field, at point E the field is transverse, and at point F there is an antiparallel component. At point D the Faraday rotation is building up clockwise and the polarization of the signal is nearly linear. Approaching E, the polarization of the signal changes from elliptical to circular, while

the Faraday rotation (determined by the position of the major axis of the ellipse) continues to build up clockwise. E is but a point in space and not a region, so no Faraday rotation is built up there. Just below E there must be an elliptical component to the polarization. The phase of each characteristic wave is continuously varying across E, so there can be no discontinuity in the Faraday rotation at E. However, there is a reversal in the direction of the longitudinal component of the magnetic field beyond E, i.e., there is an antiparallel component of the field. Hence the ordinary wave describes a left-hand helix (actually elliptical rather than circular), the extraordinary wave describes a right-hand helix, and the Faraday rotation builds up counterclockwise. Therefore, the total rotation of the wave at the receiver is the sum of the clockwise rotation from T to E and the counterclockwise rotation from E to F. This sum can be a net clockwise rotation, zero, or a net counterclockwise rotation.

The Faraday rotation is usually described by the equation:

$$\Omega = \frac{1}{2} (P_o - P_x), \tag{1}$$

where P_o and P_x are the phase path lengths (in wave lengths) of the ordinary and extraordinary waves respectively and Ω is the Faraday rotation in cycles;

$$P_o = \frac{1}{\lambda} \int_{S_o} \mu_o \, ds_o, \; P_x = \frac{1}{\lambda} \int_{S_x} \mu_x \, ds_x , \tag{2}$$

where λ is the free space wave length of the transmitted radiation, μ_o and μ_x are the indices of refraction of the ordinary and extraordinary waves respectively, and the integrals are along the ray paths from the transmitter to the receiver. Whenever the transmitted frequency is higher than the plasma frequency and collision effects are negligible, the plus sign in the Appleton-Hartree equation is used for the ordinary wave and the minus sign for the extraordinary wave. In this case μ_o is always greater than or equal to μ_x, so that $P_o \geq P_x$ and by Equation (1), $\Omega \geq 0$. Equation (2) does not indicate whether the waves describe right or left-hand helices and give only the absolute number of wave lengths. Hence Equation (1) gives the sum of the absolute values of the clockwise and counterclockwise rotation, which is not indicative of the total rotation between the transmitter and receiver.

The deficiency in Equations (1) and (2) can be corrected by defining the spatial rotation in one direction, say counterclockwise, to be positive. With this definition, when a component of the magnetic field is parallel to the ray path (as in vertically downward propagation in the northern hemisphere), the ordinary wave is negative (clockwise), the extraordinary wave is positive (counterclockwise), and the total rotation is negative (clockwise). When there is an antiparallel component of the magnetic field, all three are reversed.

Also Equations (1) and (2) then become:

$$\Omega = \frac{1}{2} (P_o + P_x) \tag{3}$$

$$P_o = \frac{1}{\lambda} \int_{S_o} - \delta \mu_o \, ds_o \qquad P_x = \frac{1}{\lambda} \int_{S_x} \delta \mu_x \, ds_x \tag{4}$$

where $\delta = + 1$ when the ray path is parallel to the longitudinal component of the magnetic field and $\delta = - 1$ when the ray path is antiparallel to the field. In the case illustrated by Figure 1D, $\delta = + 1$ from T to B and $\delta = - 1$ from B to R.

In practice, it would be difficult to do ray tracing with the use of Equations (3) and (4). This is because it would be necessary to determine the transverse point within one wave length of the transmitted radiation on both the ordinary and extraordinary ray paths in order for the resulting Faraday rotation to be accurate to within one cycle. In a ray tracing program such as described by Lawrence and Posakony (1961) or Dulk and Dean (1962), this would require layer thicknesses near the transverse point of about 6 meters for a 54 mc. signal. Round-off errors for these small layers, as well as the possible non-convergence of the iteration process for computing refraction, would make the procedure impractical. Therefore, another scheme has been devised for ray tracing in the transverse region. Advantage is taken of the facts that magnetoionic splitting is a minimum for nearly transverse propagation and that the "no magnetic field" ray path is between the ordinary ray path and the extraordinary ray path, so that least error is introduced by tracing along the "no magnetic field" ray path. The Faraday rotation is computed with the equation:

$$\Omega = \frac{1}{2\lambda} \int_S - \delta \, (\mu_o - \mu_x) \, ds \qquad (5)$$

where refraction but not magnetoionic splitting is taken into account along the "no magnetic field" ray path. This equation may be used whenever the transverse point occurs somewhere along the ray path. At the transverse point, δ changes from +1 to -1. Using Equation (5), the transverse point need not be determined as closely as when using Equations (3) and (4), and the sign of Ω indicates whether the total rotation is counterclockwise or clockwise.

There are two special cases of interest. For the first, the transverse point coincides with the bottom of the ionosphere. In this case the limiting polarization of the wave is circular, and this should be noticeable on signal strength records as a decrease in depth of the Faraday nulls. This occurrence usually will not be coincident with the true zero total Faraday, which occurs when the transverse point occurs near the middle of the ionosphere. For the second case, the transverse point is at the transmitter height and the plane of polarization of the transmitted wave is in the plane of the magnetic meridian. Then only the ordinary mode will be transmitted. At the receiver the signal will be almost circularly polarized. Should the plane of polarization of the transmitted wave be perpendicular to the magnetic meridian at the transmitter, only the extraordinary mode would be transmitted and a circularly polarized signal of opposite sense of rotation would be received.

II. ANALYSIS OF ERROR INVOLVED IN VARIOUS APPROXIMATIONS

A thorough investigation was made of one satellite pass during which transverse propagation occurred. The primary purpose of the investigation was to determine the magnitude of the errors involved in making various approximations. The pass investigated was revolution 5183 of the Transit 4A satellite which was transmitting on 54 mc and 324 mc. The satellite signals were received at a low latitude receiving station. (Johnston Island, 16° N, 190° E; geomagnetic latitude 15° N.) This pass was from north to south, the closest approach of the satellite being about 500 km east of the receiver at 10:46 AM Johnston Island standard time and the satellite altitude was about 960 km. During the pass the ionosphere was relatively quiet, the geomagnetic planetary A index was 10.

FIGURE 2
SUBSATELLITE ELECTRON CONTENT
AND EFFECTIVE IONOSPHERIC HEIGHT
VS
TIME
REV. 5183, 1961 OMICRON
HYBRID DISPERSIVE DOPPLER – FARADAY METHOD

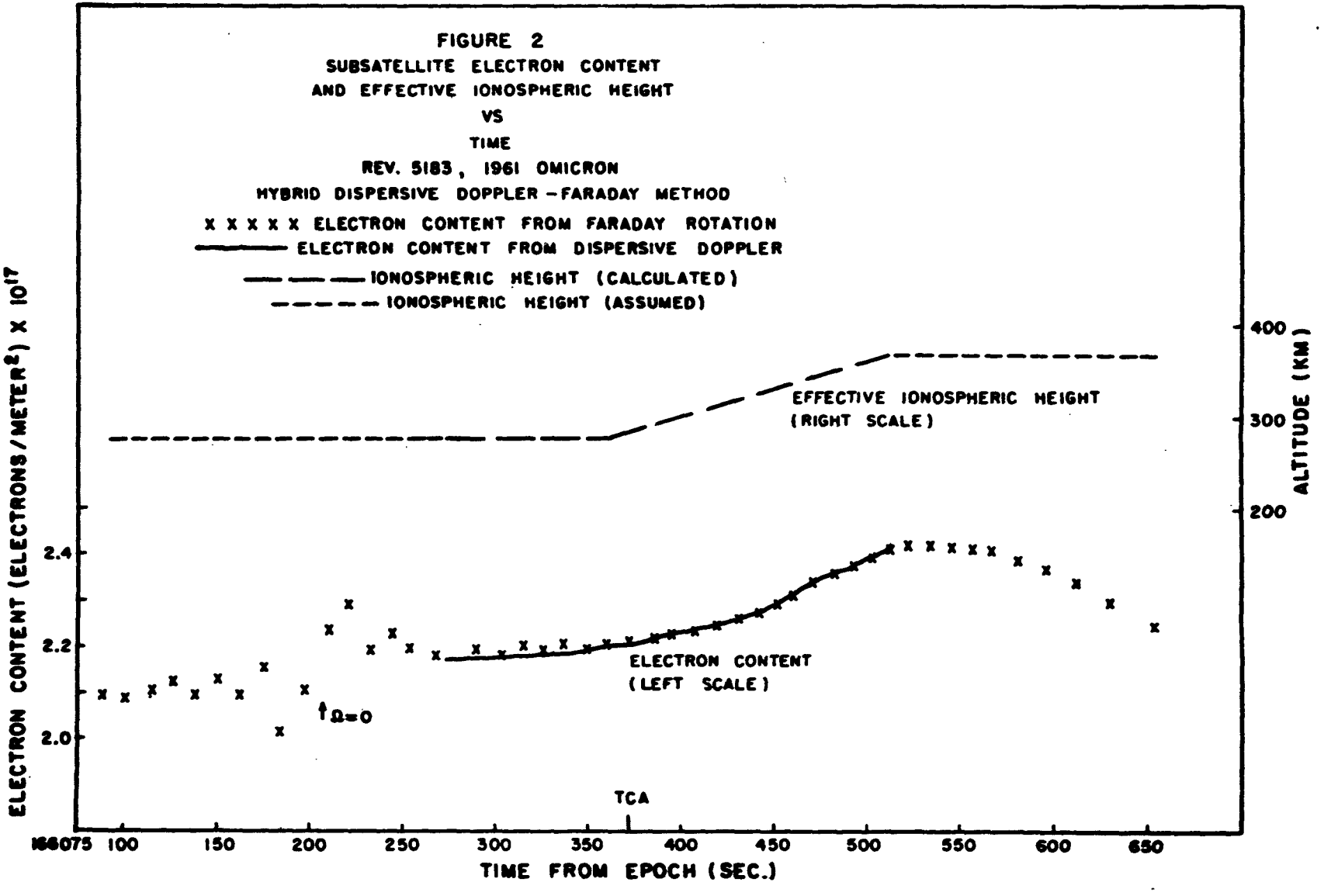

The ray tracing program used in the analysis was that of Dulk and Dean (1962). Though an option for ray tracing through an ionosphere varying in three dimensions is available in the program, computations are simplified when the ionosphere model is spherically stratified. Revolution 5183 exhibited a nearly constant subsatellite electron content over a considerable portion of the pass, enabling use of a spherically stratified ionosphere model in the ray tracing program. A preliminary investigation using the hybrid dispersive Doppler-Faraday rotation method of De Mendonca (1962) indicated that the subsatellite electron content was about 2.2×10^{17} electrons/meter^2 and that the electron content increased slightly to the south of the receiving station. Figure 2 shows the electron content profile as found by the hybrid method.

The electron density profile used was in two sections:

1. Up to H_{max}, (the height of $f2_{max}$) the profile was derived from an ionogram taken by a low latitude ionosonde (Puerto Rico) under similar ionospheric conditions.

2. Above H_{max} the profile was assumed to be that of a Chapman layer with a scale height at H_{max} of 42 km (indicated by the layer half thickness as shown on the ionogram) and a scale height gradient of .12 km/km. The Chapman scale height and scale height gradient were discussed in detail by Marks, et al, (1963), and were shown to be realistic.

For the purposes of the major part of the present investigation, the model ionosphere profile was not required to be in exact agreement with the profile actually existing at the time the satellite was tracked. It was necessary only that the same model be used in testing each of the various approximations. However, to enable comparison with measured data, it was desirable for the model profile and the actual profile to be similar in shape, and to contain the same subsatellite electron content. Therefore, the electron density model was normalized to give the subsatellite electron content of 2.2×10^{17} electron/meter^2 to be in agreement with the hybrid measurement. Also the shape of the model profile and electron density at H_{max} were later found to be in agreement with ionosonde data taken at Johnston Island during the satellite pass.

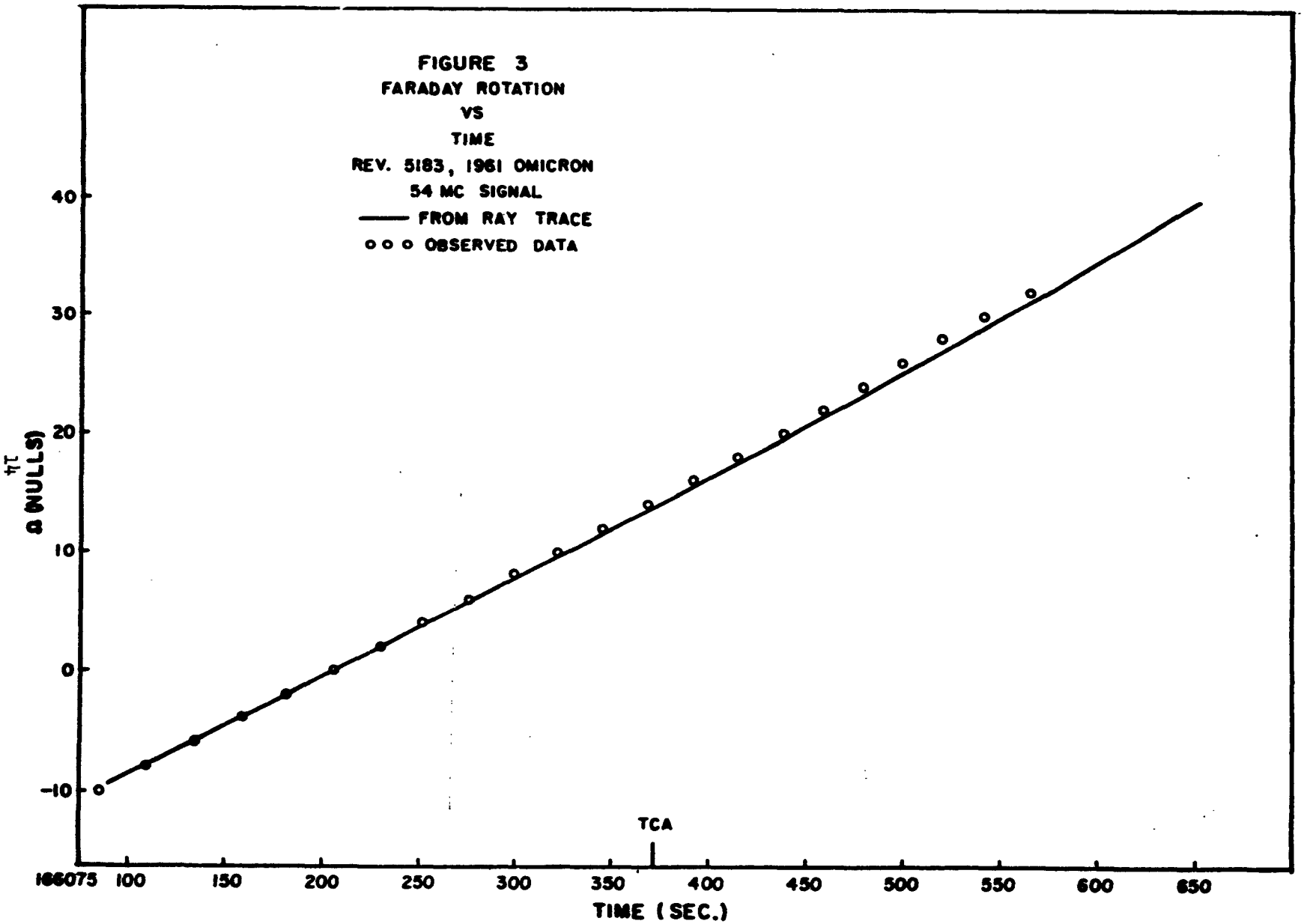
FIGURE 3
FARADAY ROTATION
VS
TIME
REV. 5183, 1961 OMICRON
54 MC SIGNAL
—— FROM RAY TRACE
o o o OBSERVED DATA
Ω (NULLS)
40
30
20
10
0
-10
TCA
166075
100
150
200
250
300
350
400
450
500
550
600
650
TIME (SEC.)

The first step in the investigation involved ray tracing the 54 mc signal from satellite to receiver at about 20 satellite locations. These locations were distributed from horizon to horizon, but the majority were in the transverse portion of the sky. In Figure 3, the Faraday rotation as computed in the ray tracing is compared with the measured Faraday rotation. Because the time of zero measured Faraday rotation cannot usually be determined from the record, it was arbitrarily chosen to be at 206 seconds, the time of zero computed Faraday. It is seen in the Figure that there is good agreement between the two sets of data over most of the interval of measurements. Only at later times, with the satellite to the south, does the measured Faraday become greater than the Faraday computed from the model, indicating increasing subsatellite electron contents to the south.

The magnetic field model used in the computations was the 6th order spherical harmonic description using coefficients of Jensen and Cain (1962) for Epoch 1960. Using this model, it was found that when signals were first received at the beginning of the pass (089 sec.), there was a transverse point along the ray path in the ionosphere at an altitude of 950 km. As the satellite traveled southward in its orbit, a transverse point continued to exist somewhere along the ray path for a period of 140 sec, during which the satellite traveled from 29.2° N, 178.4° E to 21.7° N, 181.7° E.

Figure 4 illustrates the error involved in ignoring refraction of the ray. $\Omega_{\text{st. line}}$ was obtained by using Equations (3), (4), and (5), the same equations used to obtain $\Omega_{\text{Ray Trace}}$. However, the integral was taken along the straight line path from transmitter to receiver instead of along the refracted ray paths. In all but the transverse region, the resulting error is seen in Figure 4 to be less than about 2%, with the error increasing at later times with the satellite approaching the horizon. However, near the point where $\Omega = 0$, which occurs with the transverse point at an altitude of about 340 km, ignoring refraction causes the error to be greater than 10% for a period of about 30 seconds. During the early portion of the pass, with the transverse point between 400 km and 960 km, the error is about 6%. The reason for the sensitivity to refraction effects in the transverse region is that the slight difference between the true ray direction and the straight

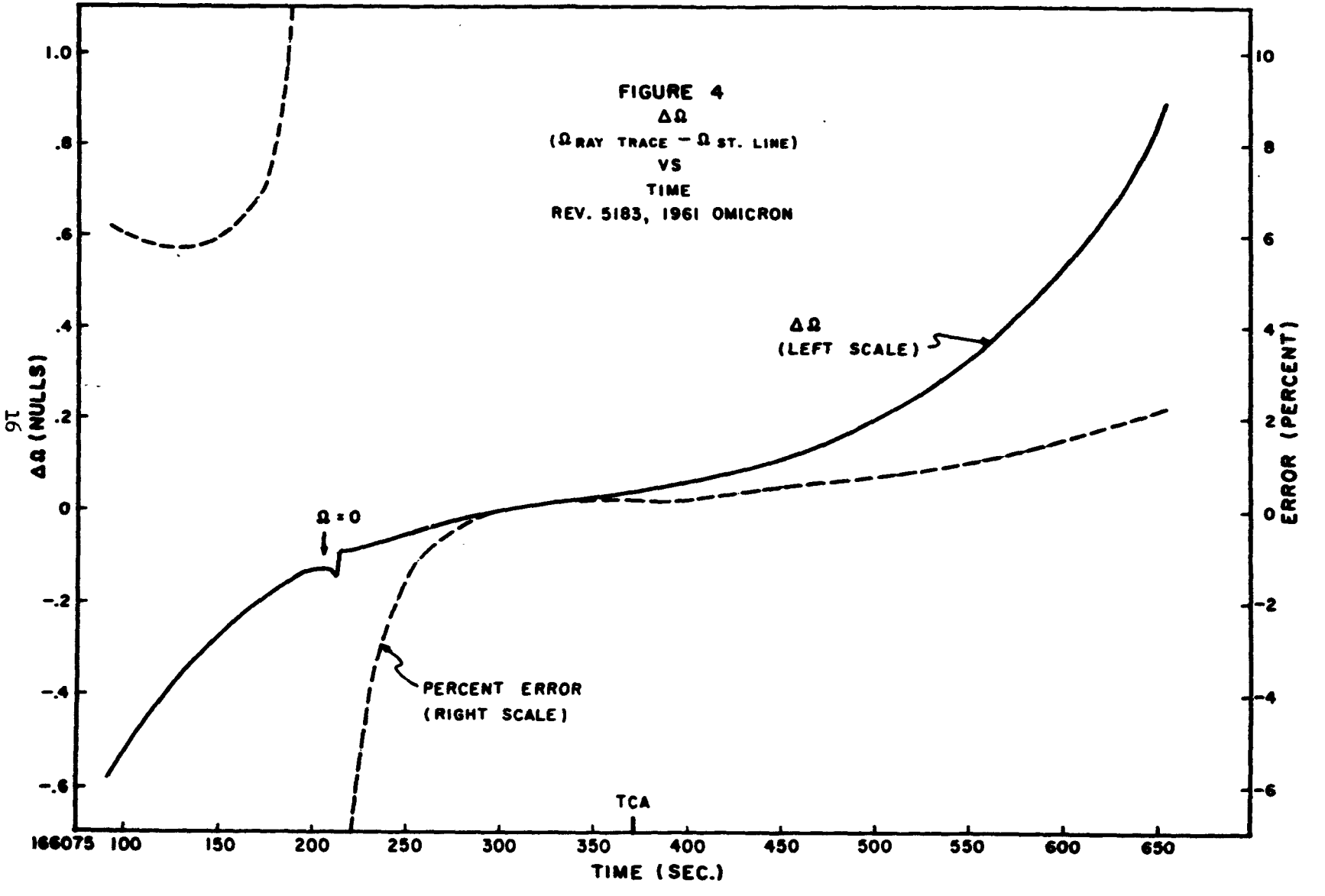
FIGURE 4
ΔΩ
(Ω RAY TRACE − Ω ST. LINE)
VS
TIME
REV. 5183, 1961 OMICRON
ΔΩ (NULLS)
ERROR (PERCENT)
ΔΩ
(LEFT SCALE)
Ω = 0
PERCENT ERROR
(RIGHT SCALE)
TCA
TIME (SEC.)
166075
1.0
.8
.6
.4
.2
0
-.2
-.4
-.6
10
8
6
4
2
0
-2
-4
-6
100
150
200
250
300
350
400
450
500
550
600
650

line path causes the transverse point to be shifted upward or downward to a considerably greater extent. The computed Faraday rotation is therefore altered by a disproportionate amount.

The error involved in using the quasi-longitudinal approximation throughout the transverse region is illustrated in Figure 5. The equation utilizing the quasi-longitudinal approximation which was used to compute the Faraday rotation is

$$\Omega_{Q.L.} = \frac{K}{f^2} \int_S H \cos\theta \, N \, ds \qquad (6)$$

where K is a constant, f is the transmitted frequency, H is the magnetic field strength, θ is the angle between the magnetic field and the wave normal, N is the electron density, and the integral is along the "no magnetic field" ray path from transmitter to receiver. The error of 1%, which is seen in Figure 5 to be nearly constant over much of the pass, can be attributed to use of a constant K which was 1% too high. Only in the ten second interval about $\Omega = 0$ is the error greater than 10%. Even in the early portion of the satellite pass, with the transverse point occurring somewhere along the ray path, use of the Q.L. approximation results in little error. Comparing Figure 4 with Figure 5, it is seen that more error is incurred in ignoring refraction than in using the Q.L. approximation, and the interval of large error is longer.

Figure 6 illustrates the error in using the Q.L. approximation along the straight line path from transmitter to receiver. The result is essentially a superposition of the errors in Figure 4 and Figure 5.

When using the Q.L. approximation above, the factor H cos θ was retained within the integral sign. Often it is desirable to find a mean value of the factor H cos θ (or H cos θ sec χ) and remove it from under the integral sign. Then Equation (6) is changed to

$$\Omega = \frac{K}{f^2} (H \cos\theta \sec\chi)_{H_i} \int_0^{H_s} N \, dh \qquad (7)$$

where H_i is the proper mean height of the ionosphere, χ is the angle between the ray path and the zenith at height H_i, and $\int_0^{H_s} N \, dh$ is the subsatellite

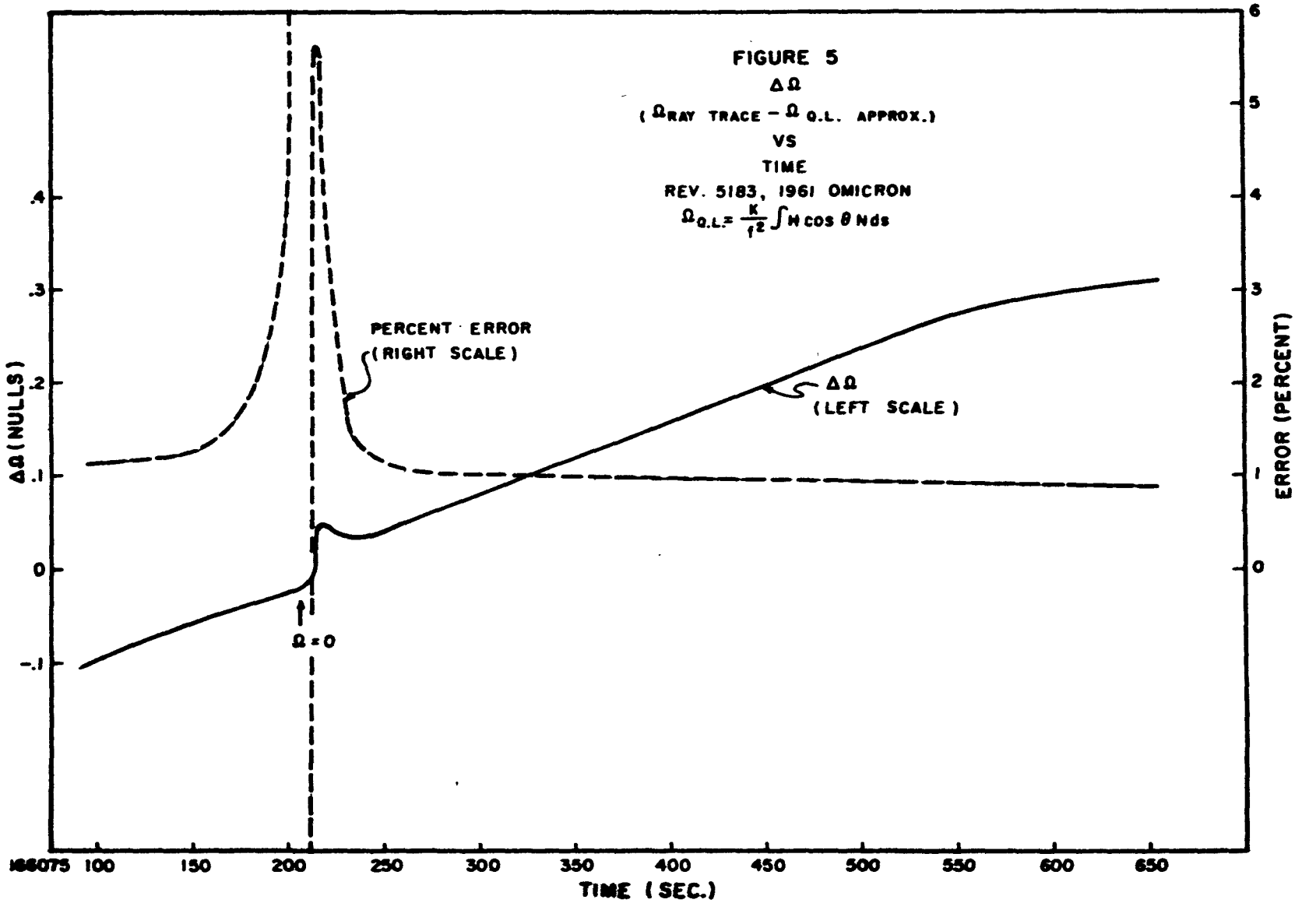
FIGURE 5
ΔΩ
(Ω RAY TRACE − Ω Q.L. APPROX.)
VS
TIME
REV. 5183, 1961 OMICRON
$\Omega_{Q.L.} = \frac{K}{f^2} \int H \cos\theta \, N ds$
PERCENT ERROR
(RIGHT SCALE)
ΔΩ
(LEFT SCALE)
Ω = 0
ΔΩ (NULLS)
ERROR (PERCENT)
TIME (SEC.)
.4
.3
.2
.1
0
-.1
6
5
4
3
2
1
0
100
150
200
250
300
350
400
450
500
550
600
650

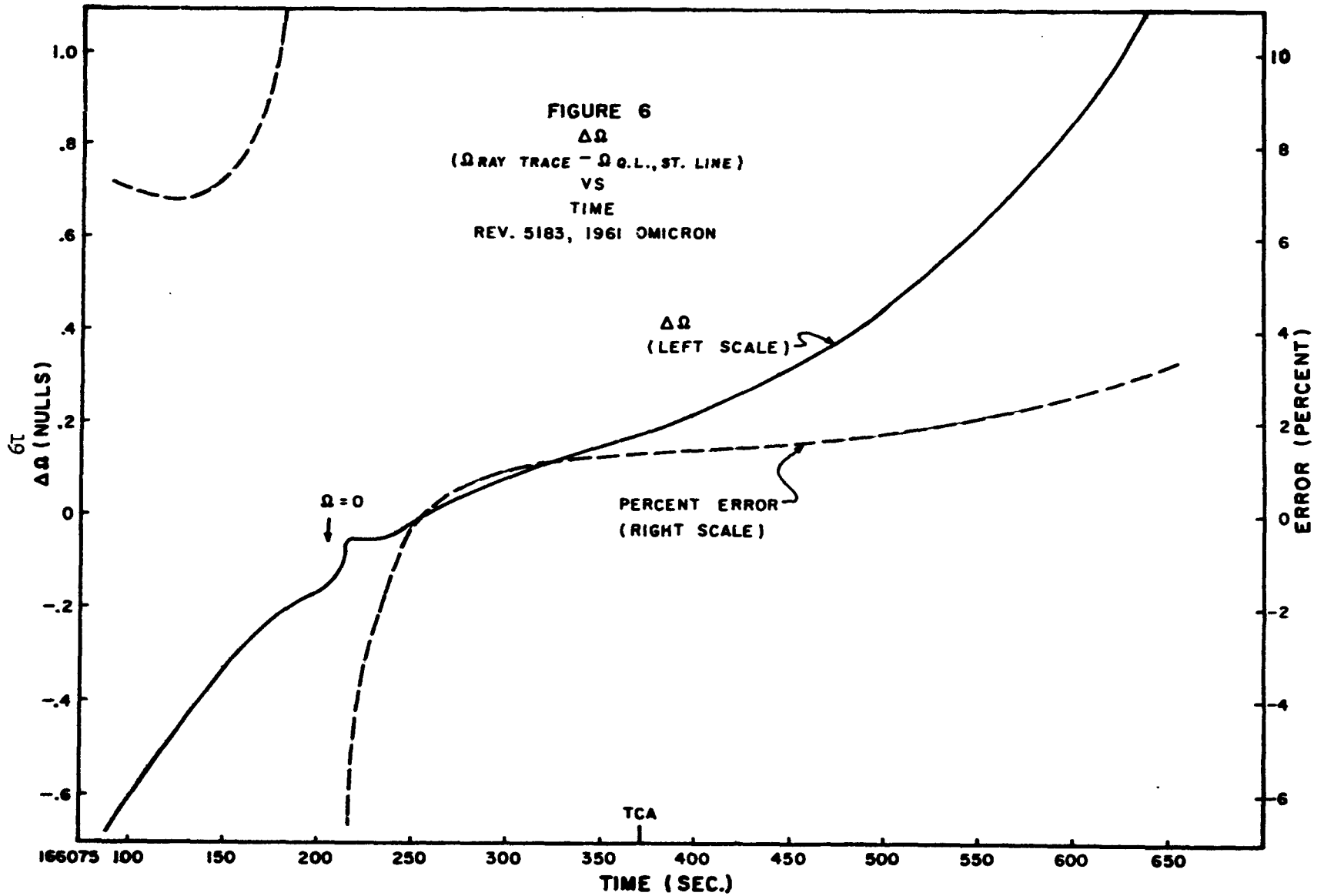
FIGURE 6
ΔΩ
(Ω RAY TRACE − Ω Q.L., ST. LINE)
VS
TIME
REV. 5183, 1961 OMICRON
ΔΩ
(LEFT SCALE)
PERCENT ERROR
(RIGHT SCALE)
Ω = 0
TCA
δτ
ΔΩ (NULLS)
ERROR (PERCENT)
TIME (SEC.)
166075
1.0
.8
.6
.4
.2
0
-.2
-.4
-.6
10
8
6
4
2
0
-2
-4
-6
100
150
200
250
300
350
400
450
500
550
600
650

electron content. Figure 7 illustrates the error resulting from use of Equation 7 when the mean or effective ionospheric height H_i is chosen to be 350 km. Again, over much of the pass the error is less than 2%. Errors of over 10% occur during an interval of about 20 seconds near the time when $\Omega = 0$. During early times the error is seen to be about 6%, with Equation 7 overestimating the rotation.

The results of assuming the mean ionospheric height to be too low, at 300 km, are shown in Figure 8. Here the error is seen to be about 4% over much of the pass, with Equation 7 overestimating the amount of Faraday rotation. Near the time when $\Omega = 0$, there is an interval of about 75 seconds when the error is greater than 40%. During early times, Equation 7 underestimated the amount of rotation by about 10%. Comparison of Figure 8 with Figure 7 shows that a mean ionospheric height of about 340 km would be the best for the particular ionospheric structure used in the computations.

The results of overestimating the mean ionospheric height by setting $H_i = 400$ km and using Equation 7 are shown in Figure 9. Again there is an error of about 4% over most of the pass, with the rotation calculated with Equation 7 being too low. Near the time when $\Omega = 0$, there is an interval of about 25 seconds when the error is greater then 40%. From the beginning of the pass until 215 seconds, an interval of about 125 seconds, the error is greater than 20%. At early times, it is seen that Equation 7 overestimates the amount of rotation.

Figure 10 is a composite of the percent errors shown in the preceding three figures. It is notable that there is a point at about 265 seconds where the Faraday rotation given by Equation 7 is independent of the altitude chosen for H_i. This is the time when the factor H cos θ sec χ changes from a decreasing function of altitude to an increasing function of altitude. Such a point has been found for all satellite passes so far investigated.

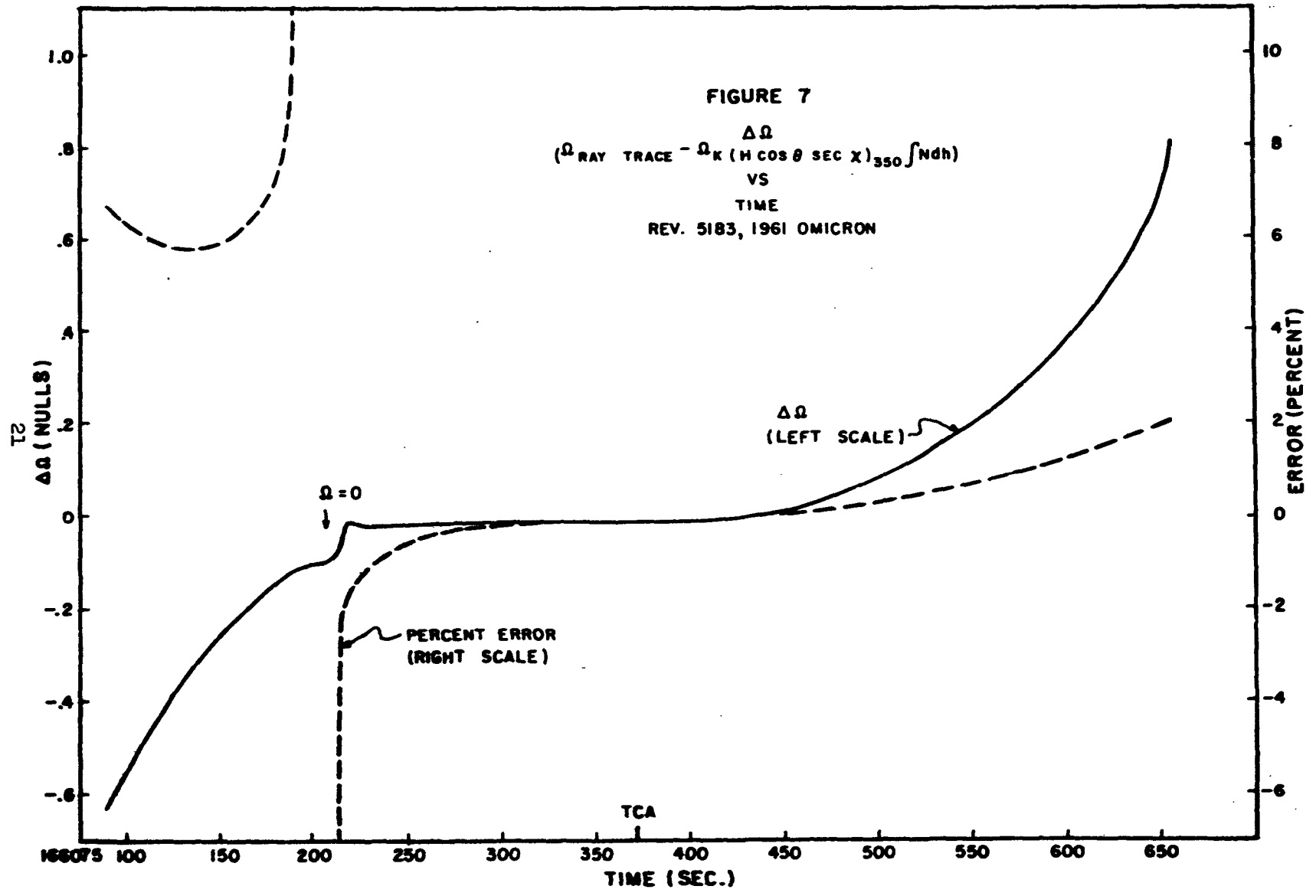
FIGURE 7
ΔΩ
(Ω RAY TRACE − Ω K (H COS θ SEC X)350 ∫Ndh)
VS
TIME
REV. 5183, 1961 OMICRON
ΔΩ (NULLS)
ERROR² (PERCENT)
ΔΩ
(LEFT SCALE)
Ω = 0
PERCENT ERROR
(RIGHT SCALE)
TCA
TIME (SEC.)
1.0
.8
.6
.4
.2
0
-.2
-.4
-.6
10
8
6
4
2
0
-2
-4
-6
100
150
200
250
300
350
400
450
500
550
600
650

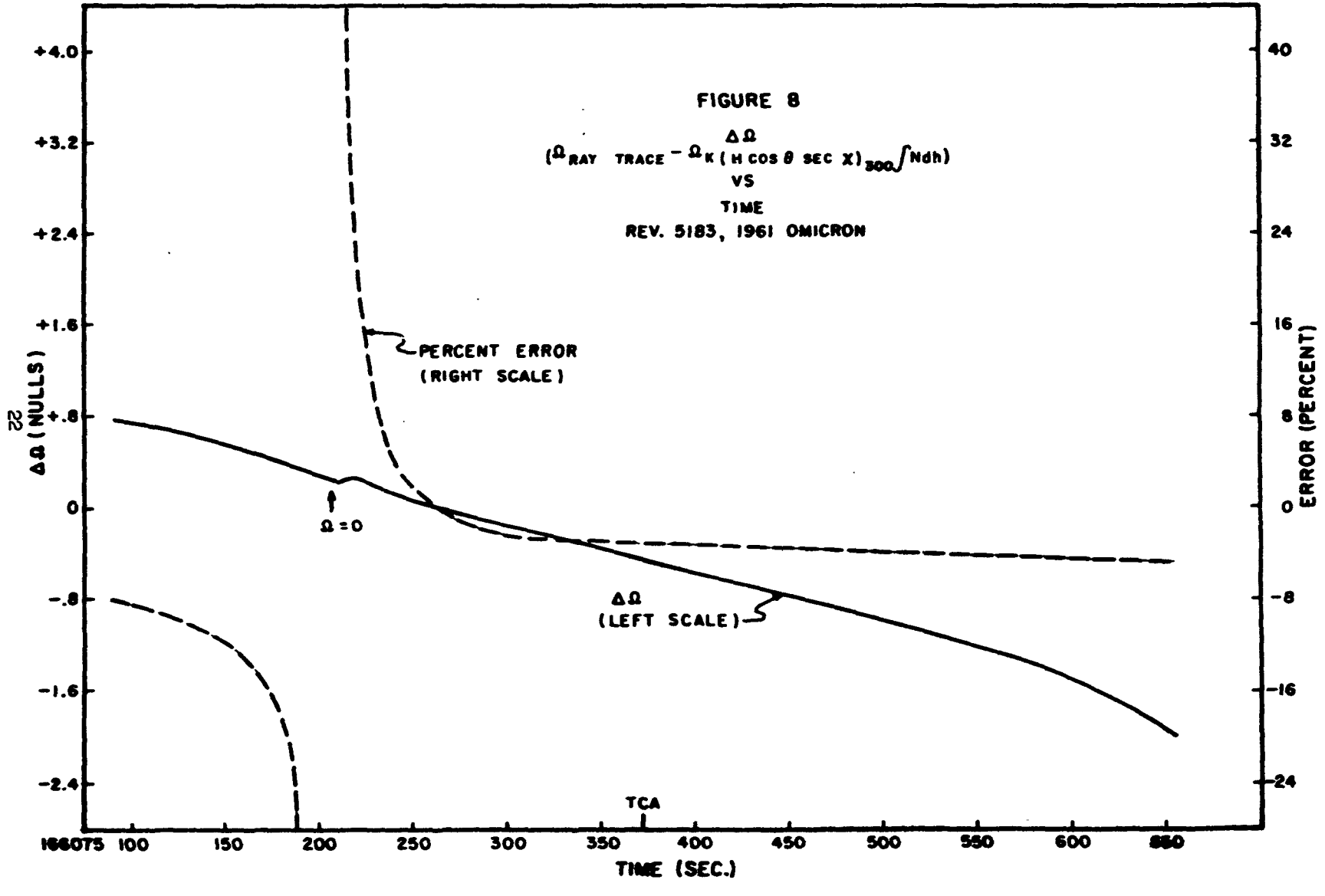
FIGURE 8
ΔΩ
(Ω RAY TRACE − Ω K (H cos θ SEC X) 300 ∫ Ndh)
VS
TIME
REV. 5183, 1961 OMICRON
PERCENT ERROR
(RIGHT SCALE)
Ω = 0
ΔΩ
(LEFT SCALE)
TCA
ΔΩ (NULLS)
ERROR (PERCENT)
TIME (SEC.)
+4.0
+3.2
+2.4
+1.6
+.8
0
-.8
-1.6
-2.4
40
32
24
16
8
0
-8
-16
-24
166075
100
150
200
250
300
350
400
450
500
550
600
650

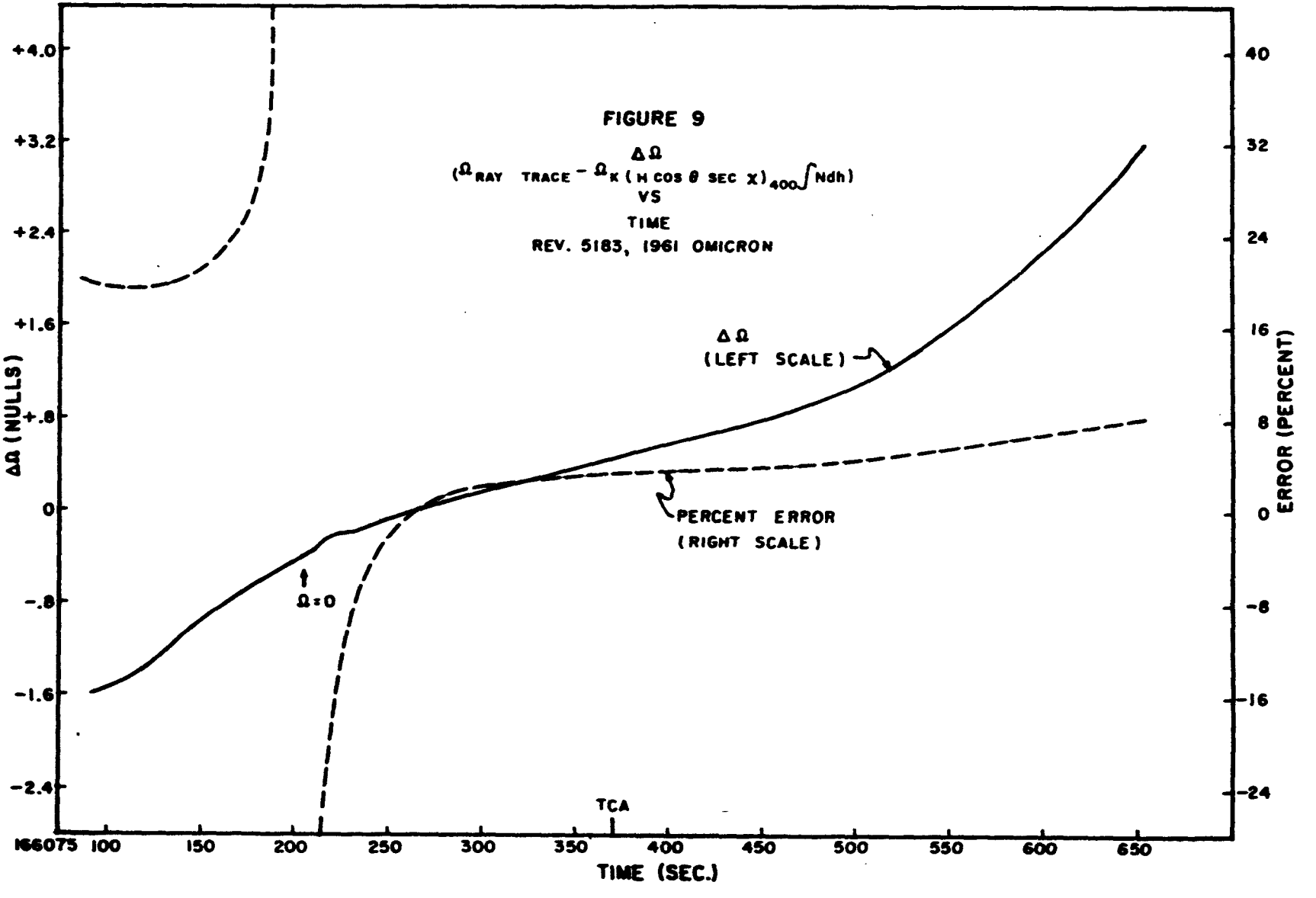
FIGURE 9
$\Delta\Omega$
($\Omega_{RAY\ TRACE} - \Omega_{K\,(H\cos\theta\ \sec\chi)_{400}\int Ndh}$)
VS
TIME
REV. 5183, 1961 OMICRON
$\Delta\Omega$
(LEFT SCALE)
PERCENT ERROR
(RIGHT SCALE)
$\Omega=0$
TCA
$\Delta\Omega$ (NULLS)
ERROR (PERCENT)
TIME (SEC.)
166075
+4.0
+3.2
+2.4
+1.6
+.8
0
-.8
-1.6
-2.4
40
32
24
16
8
0
-8
-16
-24
100
150
200
250
300
350
400
450
500
550
600
650

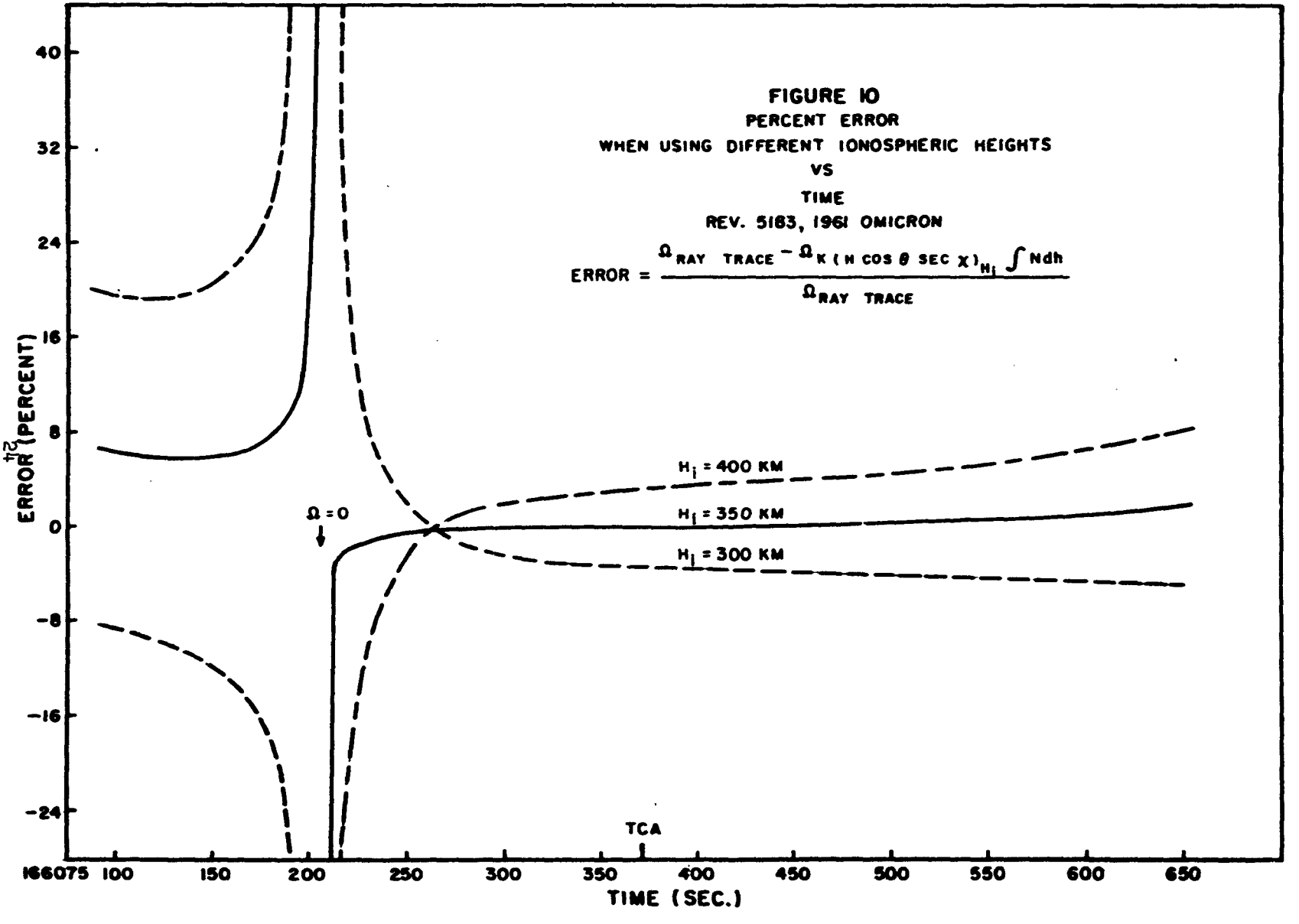
FIGURE 10
PERCENT ERROR
WHEN USING DIFFERENT IONOSPHERIC HEIGHTS
VS
TIME
REV. 5183, 1961 OMICRON
ERROR = (Ω RAY TRACE − Ω K (H COS θ SEC χ) Hi ∫ Ndh) / Ω RAY TRACE
ERROR (PERCENT)
40
32
24
16
8
0
-8
-16
-24
Ω = 0
Hi = 400 KM
Hi = 350 KM
Hi = 300 KM
TCA
166075
100
150
200
250
300
350
400
450
500
550
600
650
TIME (SEC.)

CONCLUSION

It has been shown that the usual equations for decribing Faraday rotation are incorrect whenever there is a change of sign of cos θ somewhere along the ray path. The corrected equations are given, and are shown to be consistent with measured data. Use of the uncorrected equations can lead to improper interpretation of Faraday rotation near the transverse region.

With the corrected equations used in a ray tracing program, an analysis of errors involved in several approximations shows that ignoring refraction can result in considerable error near the transverse region even at a frequency as high as 54 mc, that use of the quasi-longitudinal approximation results in less error than ignoring refraction, and that the choice of the proper mean ionospheric height is quite important when deducing ionospheric electron content from measurements of Faraday rotation.

ACKNOWLEDGMENTS

I wish to express my thanks to Mr. J. Lanahan who was largely responsible for the development of the present version of the ray tracing program; to Mr. C. L. Adams, whose section obtained the satellite data; and to Mr. I. R. Chidsey, who provided the subsatellite electron content profile. Also, I am grateful to Mr. R. S. Lawrence of the National Bureau of Standards who provided the original version of the ray tracing program and who contributed to the results in this paper through several helpful discussions.

George A. Dulk

GEORGE A. DULK
Capt, Ord Corps

REFERENCES

1. De Mendonca, F. Ionospheric Electron Content and Variations Measured by Doppler Shifts in Satellite Transmissions. Journal of Geophysical Research, 67, 6, 2315, June 1962.

2. Dulk, G. A. and Dean, W. A. Rocket and Satellite Ionosphere Studies Using Digital Ray Tracing Procedure. Ballistic Research Laboratories Report No. 1183, Aberdeen Proving Ground, Maryland, December 1962.

3. Jensen, D. C. and Cain, J. C. An Interior Geomagnetic Field. Abstract of paper presented at the 43 rd Annual Meeting of the A.G.U. Journal of Geophysical Research, 67, 9, 3568, August 1962.

4. Lawrence, R. S. and Posakony, D. J. A Digital Ray Tracing Program for Ionospheric Research. Proc. of the 2d Intl. Space Science Symposium of COSPAR. H. Kallmann ed., No. Holland Publ. Co., 1961.

5. Marks, S. T., Shafer, C. E., Cruickshank, W. J., Prenatt, R. E., and Dulk, G. A. Summary Report on Strongarm Rocket Measurements of Electron Density to an Altitude of 1500-Kilometers. Ballistic Research Laboratories Report No. 1187, Aberdeen Proving Ground, Maryland, January 1963.

DISTRIBUTION LIST

No. of Copies	Organization
20	Commander Armed Services Technical Information Agency ATTN: TIPCR Arlington Hall Station Arlington 12, Virginia
2	Director Advanced Research Projects Agency ATTN: Lt Col Roy Weidler Department of Defense Washington 25, D. C.
2	Director IDA/Weapon Systems Evaluation Group Room 1E875, The Pentagon Washington 25, D. C.
7	Chief, Defense Atomic Support Agency ATTN: Document Library Branch (5 cys) Major B. McCormac, Radiation Division Major J. E. Mock Washington 25, D. C.
1	Commanding General Field Command Defense Atomic Support Agency ATTN: Major J. G. McCray Sandia Base P. O. Box 5100 Albuquerque, New Mexico
1	Chief of Research and Development ATTN: Communications and Electronics Division Department of the Army Washington 25, D. C.
1	Commanding General U. S. Army Materiel Command ATTN: Development Division, Nuclear Branch Washington 25, D. C.
1	Commanding General U. S. Army Materiel Command ATTN: Development Division, Missile Branch Washington 25, D. C.
2	Commanding General U. S. Army Materiel Command ATTN: AMCRD-RS-PE-E AMCRD-RS-ES-A Research and Development Directorate Washington 25, D. C.
1	Commanding Officer Harry Diamond Laboratories ATTN: Technical Information Office, Branch 012 Washington 25, D. C.
1	Redstone Scientific Information Center ATTN: Chief, Document Section U. S. Army Missile Command Redstone Arsenal, Alabama
2	Commanding Officer U. S. Army Electronics R&D Activity White Sands Missile Range New Mexico
1	Chief Signal Officer Department of the Army Washington 25, D. C.
3	Commanding General U. S. Army Electronics Command Fort Monmouth, New Jersey

DISTRIBUTION LIST

No. of Copies	Organization
1	Commanding Officer Office of Special Weapons Developments U. S. Combat Developments Command Fort Bliss, Texas
2	Commanding Officer Army Research Office (Durham) ATTN: Dr. Robert Mace Dr. H. Robe Box CM, Duke Station Durham, North Carolina
2	Chief of Research and Development ATTN: Atomics Office Department of the Army Washington 25, D. C.
1	Chief of Naval Research ATTN: Mr. James Winchester Department of the Navy Washington 25, D. C.
1	Commander Naval Missile Center ATTN: Code 212.11 Point Mugu, California
3	Director U. S. Naval Research Laboratory ATTN: Dr. P. Mange Dr. Philip Shapiro Technical Library Washington 25, D. C.
2	Chief of Naval Operations ATTN: Cdr W. Eaton, OP-75 Op03EG Department of the Navy Washington 25, D. C.
2	Commander Naval Ordnance Laboratory White Oak Silver Spring 19, Maryland
1	Commander U. S. Naval Ordnance Test Station ATTN: Technical Library China Lake, California
1	Commander Pacific Missile Range ATTN: Technical Library Point Mugu, California
1	Hqs., USAF (AFCIN) Washington 25, D. C.
1	Hqs., USAF (AFRDC) Washington 25, D. C.
1	Hqs., USAF (AFORQ) Washington 25, D. C.
1	Hqs., USAF (AFDAP) Washington 25, D. C.
1	Hqs., USAF (AFTAC) Washington 25, D. C.
1	Hqs., USAF ATTN: Major E. Lowry, AFRDR/NU Washington 25, D. C.
10	AFSWC ATTN: SWRPA SWRPL CO, Naval Air Special Weapons Facility SWOI SWRPR SWRPS SWRPT SWRPI SWRJ SWRP Kirtland Air Force Base New Mexico

DISTRIBUTION LIST

No. of Copies	Organization
1	Commander Air Force Office of Scientific Research ATTN: Technical Information and Intelligence Division Washington 25, D. C.
1	ARL ATTN: Mr. Cody Wright-Patterson Air Force Base Ohio
1	FTD ATTN: AFCIN 4D3, Major Pearce Wright-Patterson Air Force Base Ohio
1	ASD ATTN: WWAD, Technical Library Wright-Patterson Air Force Base Ohio
1	Office of Aerospace Research ATTN: Major Munyon Building T-D Washington 25, D. C.
1	SSD ATTN: Technical Library AF Unit Post Office Los Angeles 45, California
1	Commander 6555 Test Wing (Dev) ATTN: DWZS, Lt Col J. G. Henry Patrick Air Force Base, Florida
1	MDC Holloman Air Force Base, New Mexico
1	AFIT Wright-Patterson Air Force Base Ohio
1	AFMTC (MTASI) Patrick Air Force Base, Florida
1	AEDC Arnold Air Force Station Tullahoma, Tennessee
1	APGC (PGAPI) Eglin Air Force Base, Florida
1	RADC ATTN: RCOIL-2 Documents Library Griffiss Air Force Base, New York
1	BSD ATTN: Technical Library Norton Air Force Base, California
1	Commander Electronic Systems Division L. G. Hanscom Field Bedford, Massachusetts
3	AFSC ATTN: Capt Bay Berrier SCR DCS/R&E Andrews Air Force Base Washington 25, D. C.
7	Commander Air Force Cambridge Research Lab. ATTN: Dr. K. Champion CRT CRTPM CRZI CRZC CRZA CRRK L. G. Hanscom Field Bedford, Massachusetts

DISTRIBUTION LIST

No. of Copies	Organization
4	Scientific and Technical Information Facility ATTN: NASA Representative (S-AK/DL) Dr. Blumle Dr. R. Bordeau Dr. Martin Swetnick P. O. Box 5700 Bethesda, Maryland
2	NASA Goddard Space Flight Center ATTN: Mr. John Naugle Mr. Robert E. Bourdeau Greenbelt, Maryland
6	Director National Bureau of Standards Central Radio Propagation Lab. ATTN: Alan Shapley Dr. R. Lawrence Dr. T. Van Zandt Mr. W. Wright Dr. K. Davies Technical Library Boulder, Colorado
2	National Science Foundation ATTN: Dr. Earl Dressler Atmospheric Sciences Washington 25, D. C.
1	Director Argonne National Laboratory ATTN: Technical Library 9700 South Cass Argonne, Illinois
1	Director Oak Ridge National Laboratory ATTN: Technical Library P. O. Box "P" Oak Ridge, Tennessee
1	Brookhaven National Laboratory Technical Information Division ATTN: Classified Document Section Upton, New York
1	U. S. Atomic Energy Commission Los Alamos Scientific Laboratory ATTN: Report Librarian P. O. Box 1663 Los Alamos, New Mexico
1	University of California Lawrence Radiation Laboratory ATTN: Technical Information Div. P. O. Box 808 Livermore, California
1	U. S. Atomic Energy Commission Division of Technical Information Extension P. O. Box 62 Oak Ridge, Tennessee
1	President Sandia Corporation ATTN: Classified Document Div. Sandia Base Albuquerque, New Mexico
1	U. S. Atomic Energy Commission ATTN: Technical Reports Library Washington 25, D. C.
2	Director Armour Research Foundation ATTN: Document Library Dr. C. M. Haaland Illinois Institute of Technology Center Chicago 16, Illinois
1	Boeing Aerospace Division ATTN: Dr. E. L. Chupp Seattle, Washington
1	CONVAIR, A Division of General Dynamics Corporation ATTN: Dr. Victor Van Lint P. O. Box 1950 San Diego 12, California

DISTRIBUTION LIST

No. of Copies	Organization
1	Cornell Aeronautical Laboratory, Inc. Box 235 Buffalo 21, New York
1	Electro-Optical Systems, Inc. ATTN: Dr. Henry Richter, Jr. 125 N. Vinedo Avenue Pasadena, California
1	E. H. Plesset Associates, Inc. 1281 Westwood Boulevard Los Angeles 24, California
1	Edgerton, Germeshausen & Grier, Inc. ATTN: Dr. M. Shuler 160 Brookline Avenue Boston 15, Massachusetts
1	Geophysics Corporation of America Burlington Road Bedford, Massachusetts
1	G. C. Dewey Company 202 E. 44th Street New York, New York
4	General Electric Company Technical Military Planning Operation ATTN: Mr. Walter Hausz Dr. Walter Dudzick Dr. Roy Hendrick DASA Data Center 735 State Street Santa Barbara, California
1	Kaman Aircraft Corporation Nuclear Division ATTN: Dr. Frank Shelton Garden of the Gods Road Colorado Springs, Colorado
1	Lockheed Missiles and Space Division Technical Information Center ATTN: Dr. Roland Meyerott 3251 Hanover Street Palo Alto, California
1	Director Lincoln Laboratory ATTN: Mr. James Pannell P. O. Box 73 Lexington 73, Massachusetts
1	Mitre Corporation Middlesex Turnpike Bedford, Massachusetts
1	Republic Aviation Corporation 223 Jericho Turnpike Mineola, New York
1	Director Research Analysis Corporation ATTN: Library 6935 Arlington Road Bethesda 14, Maryland
2	The Rand Corporation ATTN: Technical Library Dr. Robert Lelevier 1700 Main Street Santa Monica, California
1	State University of Iowa Physics Department ATTN: Document Control Station for Dr. J. A. Van Allen Iowa City, Iowa
1	Director Stanford Research Institute ATTN: Document Custodian for Dr. Allen Peterson, I. G. Poppoff Menlo Park, California

DISTRIBUTION LIST

No. of Copies	Organization
1	Stanford University ATTN: Security Officer Stanford, California
1	Space Technology Laboratories, Inc. 5730 Arbor Vitae Street Los Angeles 45, California
1	University of California Lawrence Radiation Laboratory ATTN: Dr. Ken Watson Berkeley 4, California
1	Mr. Larry Brace Department of Electrical Engineering University of Michigan Ann Arbor, Michigan
1	Dr. Wolfgang Pfister Geophysics Research Directorate L. G. Hanscom Field Bedford, Massachusetts
1	Dr. Gian Carlo Rumi School of Electrical Engineering Cornell University Ithaca, New York
1	Professor A. H. Waynick Ionospheric Research Laboratory Penn State University University Park, Pennsylvania
10	The Scientific Information Officer Defence Research Staff British Embassy 3100 Massachusetts Avenue, N. W. Washington 8, D. C.
4	Defence Research Member Canadian Joint Staff 2450 Massachusetts Avenue, N. W. Washington 8, D. C.

AD ______ Accession No. ______ UNCLASSIFIED

Ballistic Research Laboratories, APG

FARADAY ROTATION NEAR THE TRANSVERSE REGION OF THE IONOSPHERE

G. A. Dulk

BRL Report No. 1200 April 1963

RDT & E Project No. 1A011001B021

UNCLASSIFIED Report

Ionosphere - Electromagnetic effects

Faraday rotation - Mathematical analysis

It is shown that some of the equations usually used to describe Faraday rotation are incorrect for the case of propagation through an anisotropic magnetic field when the cosine of the angle between the magnetic field and the wave normal changes sign along the ray path. Such a case is common when transmissions are from a high altitude satellite in the region of the ionosphere where the direction of propagation is nearly perpendicular to the earth's magnetic field. Use of the uncorrected equations can result in misinterpretation of the data. The corrected equations are given and are shown to be consistent with measured Faraday rotation. With the corrected equations used in a ray tracing program, an analysis is made of errors resulting from the use of several approximations near the transverse region. The approximations investigated are: (1) quasi-longitudinal propagation, (2) straight line propagation, and (3) use of an effective ionospheric height.

AD ______ Accession No. ______ UNCLASSIFIED

Ballistic Research Laboratories, APG

FARADAY ROTATION NEAR THE TRANSVERSE REGION OF THE IONOSPHERE

G. A. Dulk

BRL Report No. 1200 April 1963

RDT & E Project No. 1A011001B021

UNCLASSIFIED Report

Ionosphere - Electromagnetic effects

Faraday rotation - Mathematical analysis

It is shown that some of the equations usually used to describe Faraday rotation are incorrect for the case of propagation through an anisotropic magnetic field when the cosine of the angle between the magnetic field and the wave normal changes sign along the ray path. Such a case is common when transmissions are from a high altitude satellite in the region of the ionosphere where the direction of propagation is nearly perpendicular to the earth's magnetic field. Use of the uncorrected equations can result in misinterpretation of the data. The corrected equations are given and are shown to be consistent with measured Faraday rotation. With the corrected equations used in a ray tracing program, an analysis is made of errors resulting from the use of several approximations near the transverse region. The approximations investigated are: (1) quasi-longitudinal propagation, (2) straight line propagation, and (3) use of an effective ionospheric height.

AD ______ Accession No. ______ UNCLASSIFIED

Ballistic Research Laboratories, APG

FARADAY ROTATION NEAR THE TRANSVERSE REGION OF THE IONOSPHERE

G. A. Dulk

BRL Report No. 1200 April 1963

RDT & E Project No. 1A011001B021

UNCLASSIFIED Report

Ionosphere - Electromagnetic effects

Faraday rotation - Mathematical analysis

It is shown that some of the equations usually used to describe Faraday rotation are incorrect for the case of propagation through an anisotropic magnetic field when the cosine of the angle between the magnetic field and the wave normal changes sign along the ray path. Such a case is common when transmissions are from a high altitude satellite in the region of the ionosphere where the direction of propagation is nearly perpendicular to the earth's magnetic field. Use of the uncorrected equations can result in misinterpretation of the data. The corrected equations are given and are shown to be consistent with measured Faraday rotation. With the corrected equations used in a ray tracing program, an analysis is made of errors resulting from the use of several approximations near the transverse region. The approximations investigated are: (1) quasi-longitudinal propagation, (2) straight line propagation, and (3) use of an effective ionospheric height.

AD ______ Accession No. ______ UNCLASSIFIED

Ballistic Research Laboratories, APG

FARADAY ROTATION NEAR THE TRANSVERSE REGION OF THE IONOSPHERE

G. A. Dulk

BRL Report No. 1200 April 1963

RDT & E Project No. 1A011001B021

UNCLASSIFIED Report

Ionosphere - Electromagnetic effects

Faraday rotation - Mathematical analysis

It is shown that some of the equations usually used to describe Faraday rotation are incorrect for the case of propagation through an anistropic magnetic field when the cosine of the angle between the magnetic field and the wave normal changes sign along the ray path. Such a case is common when transmissions are from a high altitude satellite in the region of the ionosphere where the direction of propagation is nearly perpendicular to the earth's magnetic field. Use of the uncorrected equations can result in misinterpretation of the data. The corrected equations are given and are shown to be consistent with measured Faraday rotation. With the corrected equations used in a ray tracing program, an analysis is made of errors resulting from the use of several approximations near the transverse region. The approximations investigated are: (1) quasi-longitudinal propagation, (2) straight line propagation, and (3) use of an effective ionospheric height.